Glutamate 270 plays an essential role in K^+-activation and domain closure of *Thermus thermophilus* isopropylmalate dehydrogenase

Éva Gráczer[1], Anna Palló[2,§,‡,&], Julianna Oláh[3], Tamás Szimler[1], Petr V. Konarev[4,$], Dmitri I. Svergun[4], Angelo Merli[5], Péter Závodszky[1], Manfred S. Weiss[6] and Mária Vas[1,*]

[1]Institute of Enzymology, Research Centre for Natural Sciences, Hungarian Academy of Sciences, Magyar tudósok krt. 2., H-1117 Budapest, Hungary.

[2]Institute of Organic Chemistry, Research Centre for Natural Sciences, Hungarian Academy of Sciences, Magyar tudósok krt. 2., H-1117 Budapest, Hungary.

[3]Department of Inorganic and Analytical Chemistry, Budapest University of Technology and Economics, Gellért Square 4., H-1111 Budapest, Hungary

[4]European Molecular Biology Laboratory, Hamburg Outstation, Notkestrasse 85, 22603 Hamburg, Germany

[5]Universitá degli Studi di Parma, Dipartimento di Bioscienze, Viale G.P. Usberti 23/A, I-43100 Parma, Italy.

[6]Helmholtz-Zentrum Berlin für Materialien und Energie, Macromolecular Crystallography (HZB-MX), Albert-Einstein-Str. 15, D-12489 Berlin, Germany

Present Addresses: [§]Structural Biology Research Center, VIB, 1050 Brussels, Belgium; [‡]Brussels Center for Redox Biology, 1050 Brussels, Belgium; [&]Structural Biology Brussels Laboratory, Vrije Universiteit Brussel, 1050, Brussels, Belgium; [$]Laboratory of reflectometry and small-angle scattering, Institute of Crystallography RAS, Leninsky pr. 59, 119333 Moscow, Russia

[*]*Corresponding author*: Mária Vas
Institute of Enzymology, Research Centre for Natural Sciences, Hungarian Academy of Sciences
H-1117 Budapest, Magyar tudósok krt. 2., Hungary
Phone: +36 1 3826 773
E-mail: vas.maria@ttk.mta.hu

Keywords: isopropylmalate dehydrogenase, activation by K^+, site-directed mutagenesis, X-ray crystallography, SAXS, FRET

ABSTRACT

The mutant E270A of *Thermus thermophilus* 3-isopropylmalate dehydrogenase exhibits largely reduced (~1%) catalytic activity and negligible activation by K^+ compared to the wild-type enzyme. A 3-4 kcal/mol increase in the activation energy of the catalysed reaction upon this mutation could also be predicted by QM/MM calculations. In the X-ray structure of the E270A mutant a water molecule was observed to take the place of K^+. SAXS and FRET experiments revealed the essential role of E270 in stabilisation of the active domain-closed conformation of the enzyme. In addition, E270 seems to position K^+ into close proximity of the nicotinamide ring of NAD^+ and the electron-withdrawing effect of K^+ may help to polarize the aromatic ring in order to aid the hydride-transfer.

Abbreviations:

IPMDH: 3-isopropylmalate dehydrogenase (EC 1.1.1.85)

Tt: Thermus thermophilus

IPM: (2*R*,3*S*)-3-isopropylmalate

MOPS: 3-(N-morpholino)-propane-sulphonic acid

SAXS: small angle X-ray scattering

FRET: fluorescence resonance energy transfer

INTRODUCTION

3-Isopropylmalate dehydrogenase (IPMDH) belongs to the class of β-hydroxyacid oxidative decarboxylases and catalyses the oxidation and decarboxylation of (2*R*,3*S*)-3-isopropylmalate (IPM) to 2-oxo-4-methyl-pentanoate (isocaproic acid) in the presence of NAD^+ and a divalent cation (Mn^{2+} or Mg^{2+}) in the leucine biosynthetic pathway of bacteria [1]. Since the chemical mechanisms of the catalysed reactions are similar, the architecture of the active sites of this class of enzymes is also very similar [2]. Yet, there are also notable differences in their functional properties, e.g. monovalent cations K^+ and NH_4^+ activate IPMDH [3,4] and tartrate dehydrogenase [5], respectively, while isocitrate dehydrogenase is insensitive of their presence [6]. In the crystal structure of the quaternary complex of *Tt*-IPMDH-Mn^{2+}-IPM-NADH a bound K^+-ion was observed in the active site [7]. Among the ligands coordinating K^+-ion the side-chain of E270 (Fig. 1A) seems to play a peculiar role. This glutamate is a conserved residue throughout in all oxidative decarboxylases, but its exact role in function has not been established, yet. In the present study E270 of Tt IPMDH was replaced by alanine in order to investigate its role in the function and activation of the enzyme by K^+.

MATERIALS and METHODS

Enzymes and chemicals

E270 of *Tt*-IPMDH was mutated into Ala using the QuickChange site-directed mutagenesis kit. The modified enzyme was expressed and purified using the previously published method applied for the wild-type enzyme [8]. The enzyme (about 30 mg/ml) was obtained in a 25 mM MOPS/KOH buffer, pH 7.6 and then lyophilized. 3-Isopropylmalic acid (IPM) was purchased from Wako Biochemicals

(Japan), NAD and NADH were Sigma products. All other chemicals were commercially available high purity grade products.

Crystallisation and X-ray analysis of E270A mutant of Tt-IPMDH

Pure lyophilized mutant (E270A) of *Tt*-IPMDH was dissolved in distilled water. Crystals were obtained using the hanging drop method at 20°C by mixing 1 µl protein solution consisting of 20 mg/ml protein, 13 mM $MnCl_2$, 9 mM IPM and 5 mM NADH with 1 µl reservoir solution consisting of 20% (w/v) PEG 6000, 0.1 M MOPS/KOH pH 7.6, and 10% (v/v) ethanol. The initial concentration of K^+ in the droplet can be estimated to be about 30 mM. Diffraction data to 2.0 Å resolution were collected from a single crystal on beamline BL14.1 of the Helmholtz-Zentrum Berlin (Germany) [9]. Data were processed using XDS [10] and the structure was determined using MOLREP [11] and the quaternary complex structure of *Tt*-IPMDH-Mn^{2+}-IPM-NADH [7] (PDB entry 4F7I) as a search model. Atomic coordinates were refined using REFMAC5 [12] and manually inspected using COOT [13]. All relevant statistics are presented in Table 1. The refined structure and the corresponding structure factor amplitudes were deposited to the PDB under the accession code 4WUO.

QM/MM modelling of the redox-reaction catalysed by IPMDH in the absence of the side-chain of E270

In order to ensure maximum comparability with our previous computational results, the Mn^{2+}-ion bound generated intermediate structures were taken from that study [7] and the side chain of the E270 amino acid was mutated *in silico* to alanine. Bound K^+-ions were removed and calculations were performed with and without the bound water molecule found in the place of K^+ in the crystal structure of the E270A mutant. In the previous study three different atom-partitioning schemes

(QM1-3) were tested [7]. Here we used QM2 of the previous study as the QM region in the calculation. All modelling details were exactly the same as in the previous study. The activation energy of the hydride transfer reaction with and without the bound water molecule was determined using 3-3 QM/MM energy profiles. Final energies published herein were determined at the B3LYP/6-311+G*/MM level of theory.

Enzyme activity measurements

Activity of IPMDH (wild type: 6-12 μg/ml, i.e., 0.16-0.32 μM monomer, or E270A mutant: 2.1 mg/ml, i.e., 55 μM) was assayed in the presence of 0.5 mM IPM, 0.5 mM $MnCl_2$ and 4 mM NAD^+ in 25 mM MOPS/KOH buffer (pH 7.6). Formation of NADH was recorded spectrophotometrically at 340 nm at 20 ^oC using a Jasco (Tokyo, Japan) V-550 spectrophotometer equipped with a Grant Y6 thermostat. Under these conditions the k_{cat} values of the wild-type and E270A mutant IPMDH active sites were 238 ± 30 and 1.09 ± 0.3 min^{-1}, respectively. Alternatively, activities were tested in 25 mM MOPS/NaOH buffer (pH 7.6) at various concentrations of added KCl. The activating effect of K^+ characterised by its activation (K_A) constant. This value has been determined by fitting the kinetic data using the equation:

$$\frac{v_{act}}{v_0} = \frac{K_A + V_{max,rel} \cdot [Me]}{K_A + [Me]} \qquad \text{(Eq. 1)}$$

where v_0 and v_{act} are velocities of the reaction in the absence and in the presence of the activator, respectively; K_A is the activation constant of metal ion, that numerically equals to the [Me] causing 50% increase of $V_{max,rel}$; [Me] is the concentration of metal ion; $V_{max,rel}$ is the maximum relative activation, i.e. the ratio of the maximal activity in the presence and in the absence of the activator.

FRET measurements

The fluorescence resonance energy transfer (FRET) between Trp(s) of IPMDH and the bound NADH was recorded at 20 ^{o}C in the presence of Mg^{2+} and IPM as reported by Dean and Dvorak [14] using a SPEX Fluoromax-3 spectrofluorimeter equipped with a Peltier thermostat (Edison, NJ). The usual mixture contained 12 μg/mL (0.32 μM monomer) IPMDH (wild-type or E270A), 12 μM NADH, 3 mM $MgCl_2$ and 1 mM IPM. The protein was excited at 295 nm and the emission by the bound NADH was recorded between 300 and 550 nm in a cuvette with 10 mm path length. The slits of 2 and 4 nm were applied for excitation and emission, respectively. All measurements were carried out in the presence of various concentrations of KCl.

SAXS measurements and data processing

Synchrotron radiation X-ray scattering data were collected on the P12 beam line at the Hamburg EMBL Outstation (on the PETRA III storage ring, at DESY). Solutions of both wild type and E270A mutant of *Tt* IPMDH, their complexes with Mn^{2+}, IPM and NADH (non-functioning complex) in 25 mM MOPS/NaOH buffer, pH 7.6, without and with added KCl (cf. Table 3), measured at protein concentrations in the range from 5.0 to 10 mg/ml using pixel 2M PILATUS detector (DECTRIS, Switzerland) at a sample-detector distance of 3.1 m, and wavelength λ = 1.25 Å, covering the momentum transfer range $0.01 < s < 0.45$ Å^{-1} ($s = 4\pi \sin(\theta)/\lambda$ where 2θ is the scattering angle). The concentrations of Mn^{2+}, IPM and NADH in the protein samples were 1 mM, 0.5 mM and 5 mM, respectively. To check for radiation damage, twenty 50-ms exposures were compared; no radiation damage effects were observed. The data, after normalization to the intensity of the incident beam, were averaged, and the scattering of the buffer was subtracted. All data manipulations were performed using the program package PRIMUS [15].

Structural parameters, the forward scattering I(0) and the radius of gyration R_g were evaluated using the Guinier approximation [16] and the program GNOM [17]. The radii of gyration and the scattering patterns from the crystallographic models of wild type apo *Tt* IPMDH (pdb:

2Y3Z) and its substrate complex with Mn^{2+}, IPM and NADH (pdb: 4F7I) were computed using the program CRYSOL [18]. The program OLIGOMER [15] was used to calculate the ratio of open- and closed-form species present in *Tt* IPMDH solutions as described in [19].

RESULTS and DISCUSSION

No K^+-binding is observed in the X-ray structure of E270A mutant

The global structure of E270A mutant IPMDH with bound Mn^{2+}, IPM and NADH exhibits a closed conformation, but slightly less closed than that of the previously determined [7] wild-type enzyme. However, the active sites exhibit well defined differences due to the mutation. Fig. 1 illustrates part of the active site of *Tt*-IPMDH with bound IPM and NADH both of the wild-type (A) and the E270A mutant (B) enzymes. In the wild-type enzyme the carboxylate group of E270 is an important electrostatic ligand for K^+-ion. In the active site of the wild-type IPMDH there was a peak observed on the F_o-F_c difference density map when the K^+ ion was initially modelled as water, however in case of the E270A mutant enzyme there was no residual density when this peak was modelled as water. Furthermore, chemistry also implies a different species. In the crystal structure of the wild-type enzyme the partially negatively charged carbonyl of Gly70 coordinates the K^+-ion, while in the absence of the charged ion, in case of the E270A mutant, the density map shows this carbonyl group facing the other direction (cf. Fig. 1B) and making a water bridged H-bonding interaction (not shown) towards nicotinamid moiety of NADH.. Thus, one can assume that E270A mutant lacks the ability of K^+-binding.

Activation of IPMDH by K^+-ion and the kinetic parameters of E270A mutant

Activity of the wild-type *Tt*-IPMDH was tested both in the absence and in the presence of various concentrations of K^+-ion. Fig. 2A shows the well-pronounced activating effect of K^+-ion: it increases the k_{cat} value by more than one order of magnitude. Our previous QM/MM calculations,

indeed, have shown that the electron-withdrawing effect of K^+ may polarise the nicotinamide ring of NAD^+ at its C4-atom and thereby favour the occurrence of the hydride-transfer [7]. On the other hand, the mutant E270A IPMDH, exhibits only a very low (~1 %) activity compared to the wild type enzyme, even in the presence of high excess of K^+-ion (cf. Fig. 2B). The kinetic parameters of E270A mutant and of the wild-type enzyme are compared in Table 2. Accordingly, E270A exhibits extremely reduced affinity towards K^+-ion. The activity of E270A is reduced even in the presence of saturating concentration of K^+-ion, suggesting that the glutamate side-chain of E270 itself has some additional catalytic role. The crystal structure shows that E270 is in a direct interaction with the nicotinamide group (cf. Fig. 1A) and thereby contributes to its proper orientation for the reaction. Indeed, the K_m-value of NAD^+ is increased significantly for E270A compared to that of the wild-type enzyme (Table 2). Furthermore, as it will be shown below, the side-chain of E270 may stabilize the active closed conformation of the enzyme.

Estimated activation energy of the redox step of IPMDH catalysed reaction in case of E270A mutant

In order to estimate the activation energy of the hydride transfer reaction, 3-3 parallel QM/MM energy profile calculations were carried out for the E270A mutant enzyme with and without the bound water molecule present in the place of K^+. The presence of the water molecule had no significant influence on the obtained activation energies. In the case of the three profiles the activation energies in the mutant increased to 18.4, 21.1 and 22.2 kcal/mol, which corresponds to an increase of 3.5, 4.6 and 3.9 kcal/mol, respectively, compared to the wild-type, K^+ bound structure [7]. Based on chemical thermodynamics it can be expected that 3-4 kcal/mol increase in the activation energy decreases the reaction rate 150 to 1000 fold, which is the range for the experimentally observed 242-fold decrease in the k_{cat} value of the mutant enzyme in the absence of K^+ compared to the wild-type enzyme at saturating K^+ concentration.

Both K^+-ion and the side-chain E270 are essential for FRET-formation

It has been noted that spectral changes, characteristic of FRET from the Trp side chain(s) of IPMDH to the bound NADH can occur but, interestingly only if the substrate IPM is also bound and stabilizes the closed (active) conformational state of the enzyme [14]. On this basis FRET phenomenon of IPMDH is assumed to be a characteristics of its domain-closed conformation. Here we found that both the mutant E270A and the K^+-free wild-type enzyme exhibit only very negligible FRET spectra (Fig. 3A), that raises the possibility of the absence of domain closure in both cases. The large spectral changes observed upon addition of K^+-ion to the wild type enzyme allowed us to determine its binding constant (Fig. 3B) that is found to be K_d = 5.0±0.6 mM, i.e. in good agreement with the value of the activatory constant (K_A) determined above (Table 1). However, to test the effects of mutation (E270A) or removal of K^+ on the domain opening/closing requires more direct experiments. Therefore, SAXS-experiments have been devised.

Domain closure is prevented upon mutation of E270A

SAXS is the most appropriate method to test protein conformational changes occurring in solution, especially if it is accompanied by changes in the shape of the molecule, such as the domain closure. In our previous studies with the wild-type *Tt*-IPMDH we clearly detected domain closure in the complex with Mn^{2+} and IPM [19]. This experiment was repeated with the mutant E270A that also binds the substrate MnIPM. Table 3 summarizes the calculated *R*g values and the extent of domain closure as expressed by percentage of the open and closed forms estimated as described in the Methods. The results show that in solution E270A retains its open conformation even in the quaternary Mn-IPM-NADH-IPMDH complex, both in the presence and in the absence of K^+. Thus, in the absence of this glutamate side-chain the tertiary interactions stabilising the enzyme-closed conformation are possibly weakened. Indeed, the electrostatic interactions of the carboxylate of E270 with the side-chains of R94 and R104 that would stabilize the closed state of Hinge 1 (cf. Fig. 4) are absent in the structure of E270A mutant. Thus, the low activity of the mutant is not only due

to the weak interactions with K^+ (cf. Table 2), but also to the predominance of the open conformation, and perhaps to the slow equilibration between the open-closed forms. – It may also be noted that during the long time of crystal growing the closed conformation can be selected and the open-closed conformational equilibrium can be shifted towards this less soluble form.

The effect of K^+ on the domain closure was also investigated and, in contrast to the expectation, no significant effect was detected (Table 3). Thus, domain-closed conformation for the wild type enzyme can be formed even in the absence of K^+-ion, i.e. in the absence of formation of the FRET spectrum (Fig. 3A). It follows, therefore, that appearance of the FRET spectrum is not always an indication of the domain closured conformation, as was assumed previously. The bound K^+-ion may itself contribute to the occurrence of FRET by sensitively influencing the plane orientation of the quinoidal-ring of the bound NADH.

CONCLUSIONS

A conserved glutamate side-chain (E270) in the active site of *Tt*-IPMDH exhibits multiple roles: *i.* it is the main coordinating ligand of the activation potassium ion; *ii.* it orients properly the reacting nicotinamide ring of NAD^+ optimal for the enzymatic reduction and *iii*. it contributes to the formation of the active, closed conformation. This glutamate is conserved among the oxidative decarboxylases and its direct and/or indirect effects may be generalised.

ACKNOWLEDGEMENTS

The financial support by the grants OTKA (NK 108642) of the Hungarian National Research Fund is gratefully acknowledged. We are also grateful to the EMBL-HH (Hamburg Outstation, Germany) and HZB (Berlin) for access to their synchrotron facilities. The research leading to these results has received funding from the European Community's Seventh Framework Programme (FP7/2007-2013) under grant agreement No. 226716. D.I.S. and P.V.K. acknowledge support from the German Ministry of Education and Science (BMBF) project BIOSCAT, Grant 05K20912. A.P. gratefully acknowledges the support of M. Czugler (Research Centre for Natural Sciences, Hungarian Academy of Sciences, Budapest, Hungary) and thanks the National Science and Technology Office (Hungary) for an X-ray diffractometer purchase grant (MU-00338/2003). J.O. acknowledges the support of the János Bolyai Research Scholarship of the Hungarian Academy of Sciences.

REFERENCES

[1] Hayashi-Iwasaki, Y. and Oshima, T. (2000) Purification and characterization of recombinant 3-isopropylmalate dehydrogenases from Thermus thermophilus and other microorganisms. Methods Enzymol 324, 301-22.

[2] Aktas, D.F. and Cook, P.F. (2009) A lysine-tyrosine pair carries out acid-base chemistry in the metal ion-dependent pyridine dinucleotide-linked beta-hydroxyacid oxidative decarboxylases. Biochemistry 48, 3565-77.

[3] Sekiguchi, T., Harada, Y., Shishido, K. and Nosoh, Y. (1984) Cloning of beta-isopropylmalate dehydrogenase gene from Bacillus coagulans in Escherichia coli and purification and properties of the enzyme. Biochim Biophys Acta 788, 267-73.

[4] Yamada, T., Akutsu, N., Miyazaki, K., Kakinuma, K., Yoshida, M. and Oshima, T. (1990) Purification, catalytic properties, and thermal stability of threo-Ds-3-isopropylmalate dehydrogenase coded by leuB gene from an extreme thermophile, Thermus thermophilus strain HB8. J Biochem (Tokyo) 108, 449-56.

[5] Serfozo, P. and Tipton, P.A. (1995) Substrate determinants of the course of tartrate dehydrogenase-catalyzed reactions. Biochemistry 34, 7517-24.

[6] Miller, S.P., Goncalves, S., Matias, P.M. and Dean, A.M. (2014) Evolution of a transition state: role of lys100 in the active site of isocitrate dehydrogenase. ChemBioChem 15, 1145-53.

[7] Palló, A., Oláh, J., Gráczer, E., Merli, A., Závodszky, P., Weiss, M.S. and Vas, M. (2014) Structural and Energetic Basis of Isopropylmalate Dehydrogenase Enzyme Catalysis. FEBS J.

[8] Gráczer, É., Varga, A., Melnik, B., Semisotnov, G., Závodszky, P. and Vas, M. (2009) Symmetrical refolding of protein domains and subunits: example of the dimeric two-domain 3-isopropylmalate dehydrogenases. Biochemistry 48, 1123-34.

[9] Mueller, U. et al. (2012) Facilities for macromolecular crystallography at the Helmholtz-Zentrum Berlin. J Synchrotron Radiat 19, 442-9.

[10] Kabsch, W. (2010) Xds. Acta Crystallogr D Biol Crystallogr 66, 125-32.

[11] CCP4 (1994) The CCP4 (Collaborative Computational Project Number 4) suite: programmes for protein crystallography. Acta Crystallogr. D40, 760-763.

[12] Murshudov, G.N., Vagin, A.A. and Dodson, E.J. (1997) Refinement of macromolecular structures by the maximum-likelihood method. Acta Crystallogr D Biol Crystallogr 53, 240-55.

[13] Emsley, P. and Cowtan, K. (2004) Coot: model-building tools for molecular graphics. Acta Crystallogr D Biol Crystallogr 60, 2126-32.

[14] Dean, A.M. and Dvorak, L. (1995) The role of glutamate 87 in the kinetic mechanism of Thermus thermophilus isopropylmalate dehydrogenase. Protein Sci 4, 2156-67.

[15] Konarev, P.V., Volkov, V.V., Sokolova, A.V., Koch, M.H.J. and Svergun, D.I. (2003) *PRIMUS*: a Windows PC-based system for small-angle scattering data analysis. J. Appl. Crystallogr. 36, 1277-1282.

[16] Guinier, A. (1939) La diffraction des rayons X aux trés petits angles; application á l'étude de phénoménes ultramicroscopiques. Ann. Phys. 12, 166-237.

[17] Svergun, D.I. (1992) Determination of the regularisation parameter in indirect-transform methods using perceptual criteria. J. Appl. Crystallogr. 25, 495-503.

[18] Svergun, D.I., Barberato, C. and Koch, M.H.J. (1995) CRYSOL - a program to evaluate X-ray solution scattering of biological macromolecules from atomic coordinates. J. Appl. Crystallogr. 28, 768-773.

[19] Gráczer, É., Konarev, P.V., Szimler, T., Bacsó, A., Bodonyi, A., Svergun, D.I., Závodszky, P. and Vas, M. (2011) Essential role of the metal-ion in the IPM-assisted domain closure of 3-isopropylmalate dehydrogenase. FEBS Lett 585, 3297-302.

[20] Weiss, M.S. (2001) Global indicators of X-ray data quality. J. Appl. Cryst. 34, 130-135.

LEGENDS to the FIGURES

Fig. 1 Structural comparison of the active sites of *Tt*-IPMDH-Mn^{2+}-IPM-NADH complexes of the wild type (A) and the E270A mutant (B). K^+ is presented with a brown sphere, waters with blue, substrates as ball and stick, and all side-chains coordinating K^+ are shown as stick models coloured according to atom types. Grey ribbons represent part of the β-strand C (residues 66-72) and the nucleotide binding loop (residues 270-277). The dashed lines illustrate atomic distances smaller than 3.5 Å.

Fig. 2 Activation of IPMDH by K^+-ion. For measuring the activities of wild-type (o-o) (A) and E270A mutant (Δ-Δ) (B) IPMDHs the substrates were applied at closely saturating concentrations (cf. Methods) and the concentration of K^+-ion was varied. The activities (relative to the one in the absence of K^+-ion) are plotted against K^+-concentration. The activating constants of K^+ have been determined by fitting the continuous lines to the experimental data using Eq. 1. and summarised in Table 2.

Fig. 3 Effect of E270A mutation and the K^+-ion on the FRET spectrum of IPMDH.

A: Fluorescence emission spectra of FRET (cf. Methods) characteristic of the wild type IPMDH is recorded in the absence (dotted line) and in the presence of 100 mM K^+ (continuous line). The measurement has been repeated with the mutant E270A in the presence of 300 mM KCl (dashed line). It is noted that in the absence of K^+ the spectrum of the E270A mutant coincides with that of the wild-type enzyme (dotted line). B: Titration of the wild-type IPMDH (0.32 μM) with K^+ by the aid of the FRET signal at $\lambda_{emission}$=410 nm.

Fig. 4 Effect of E270 side-chain on the conformation of Hinge 1 of IPMDH. Constituents of Hinge 1 including α-helix d and β-strand F as well as its surroundings including the IPM and K^+

binding sites are represented by grey ribbon diagrams. The substrate IPM (ball and stick model) and the interaction side-chains (stick models) are coloured according to atom types. K^+ and Mg^{2+} ions are represented by brown and violet spheres, respectively.

Figure 1.

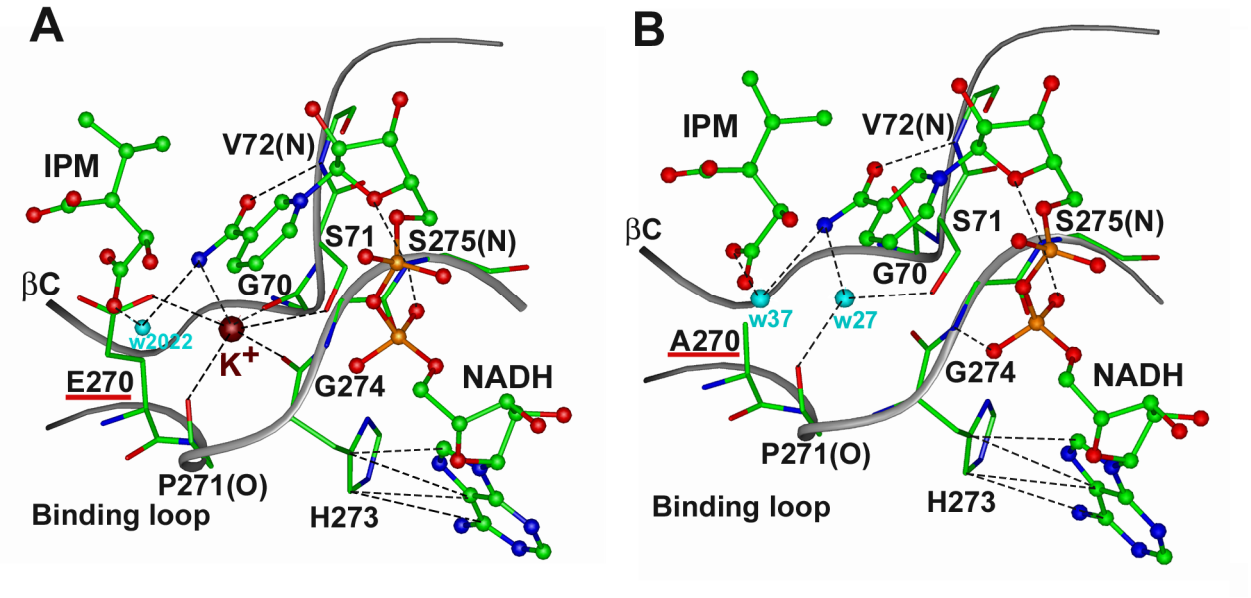
A
IPM
V72(N)
S71
S275(N)
βC
G70
w2022
K+
E270
G274
NADH
P271(O)
Binding loop
H273
B
IPM
V72(N)
βC
S71
S275(N)
G70
w37
w27
A270
G274
NADH
P271(O)
Binding loop
H273

Figure 2.

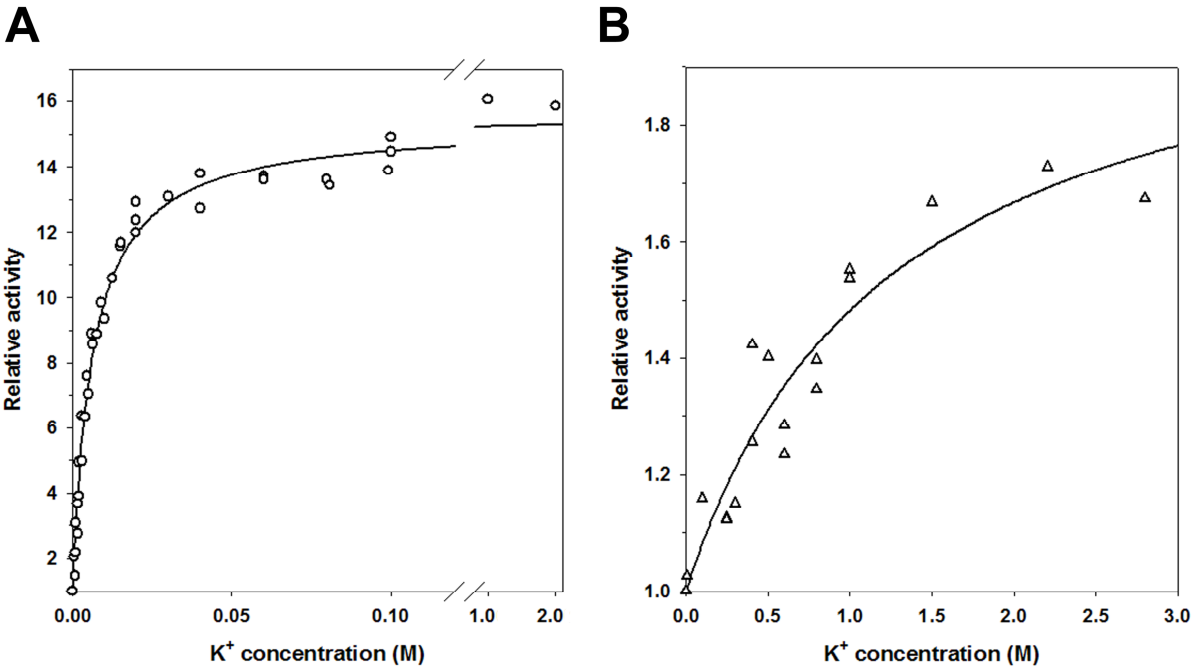
A
Relative activity
16
14
12
10
8
6
4
2
0.00
0.05
0.10
1.0
2.0
K+ concentration (M)
B
Relative activity
1.8
1.6
1.4
1.2
1.0
0.0
0.5
1.0
1.5
2.0
2.5
3.0
K+ concentration (M)

Figure 3.

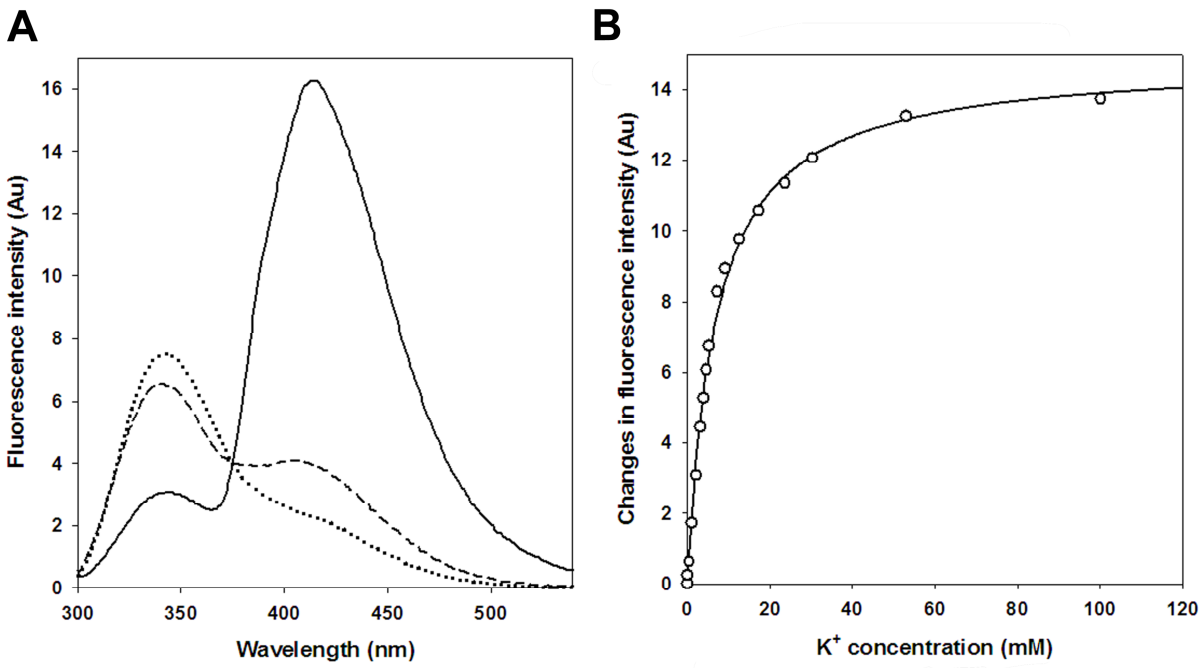
A
Fluorescence intensity (Au)
Wavelength (nm)
B
Changes in fluorescence intensity (Au)
K+ concentration (mM)

Figure 4.

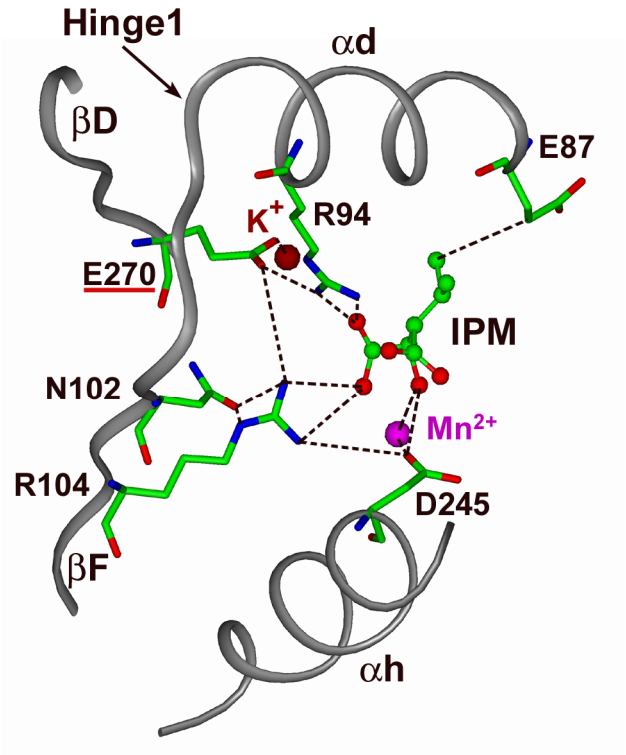

Table 1. Data collection and processing, structure-refinement and validation statistics

	4WUO
Data Collection	
Wavelength (Å)	0.91841
Crystal to detector distance (mm)	225.0
Rotation range per image (°)	0.2
Total rotation range (°)	128
Data Processing	
Space group	$C222_1$
Cell constants (Å)	50.18, 143.25, 174.89
Resolution range	41.6-2.05
last shell	2.10-2.05
Mosaicity	0.200
Completeness (%)	99.6 (97.9)
No. of observed/unique	207793/39957
(last shell)	(14280/2875)
Mean $I/\sigma(I)$	17.23 (2.71)
$R_{r.i.m.}$ [a]	0.080 (0.682)
Overall B-factor from Wilson plot (Å^2)	36.1
Optical resolution (Å)	1.64
V_M (Å^3 Da^{-1})	1.99
Solvent content (%)	38
Refinement [c]	
No. of reflections, working set	37938 (2716)
No. of reflections, test set	2009 (148)
$R_{cryst.}$	0.170
R_{free}	0.229
DPI(Å)	0.213
Number of atoms	
protein	5235
ions	3
IPM	24
NADH	88
other organic	43
water molecules	180
R.m.s. deviations	
bonds (Å)	0.015
angles (°)	1.7
Average B-factors	
protein(Å^2)	37.2
ions	33.4
IPM	28.9
NADH	28.5
other organic	47.9
water molecules	36.3
Ramachandran plot	
most favoured (%)	97.7
allowed (%)	2.3
No. of dimers / asymmetric unit	1

[a] $R_{r.i.m.} = \left(\sum \left(n/(n-1)\right)^{0.5} \sum \left|\langle I_h \rangle - I_{hj}\right|\right) / \left(\sum I_{hj}\right)$ *with* $\langle I_h \rangle = \left(\sum I_{hj}\right)/n_j$ [20]

Table 2. Kinetic constants of E270A mutant in comparison to the wild-type *Tt*-IPMDH

The kinetic measurements have been carried out as described in the Materials and Methods under the conditions specified in the Legends to Fig. 2.

Kinetic constants		Wild-type	E270A mutant
k_{cat} (min^{-1})	no K^+	15.3±4	0.95±0.2
	saturating [K^+]	238±30[2]	1.96±0.3
K^+-ion K_A[1] (mM)	varying concentrations of K^+	6.1±0.6	1240±200
IPM K_m (μM)		16±3[2]	32±5
NAD K_m (μM)	25 mM K^+	290±50	660±55
Mn^{2+} K_m (μM)		10±4[2]	25±6

[1] K_A: activatory constant
[2] These kinetic constants has been determined earlier [19]

Table 3. Comparison of SAXS experimental data with those derived from the crystallographic models.

SAXS experiments			Discrepancy values χ between the scattering from crystallographic models and experimental data			Volume fractions of open/closed structures	
Tt-IPMDH-Mn-IPM-NADH	Rg, Å [a]		Closed crystal structure	Open crystal structure	Open/closed mixture[c]	$V_{closed,}$ %	$V_{open,}$ %
	GNOM method	Guinier method					
wild-type (no K^+)	27.4±0.2	27.4±0.3	1.18	1.19	**1.09**	53±3	47±3
wild-type (50 mM K^+)	27.2±0.2	27.3±0.3	1.17	1.20	**1.11**	58±3	42±3
E270A mutant (no K^+)	28.3±0.2	28.4±0.3	2.03	**1.15**	1.14	4±3	97±5
E270A mutant (1 M K^+)	28.4±0.2	28.5±0.3	1.71	**1.08**	1.07	5±3	95±5
Rg (theoretical), angstroms [b]			26.67	28.45			
Molecular mass, kDa [b]			74.3	73.8			

[a]The R_g values were computed by two alternative methods, using the program GNOM and Guinier approximation, respectively.

[b] Radius of gyration and molecular mass of the high resolution models as retrieved from the PDB: 4F7I for the closed crystal structure of the quaternary complex of *Tt* IPMDH-Mn-IPM-NADH and 2Y3Z for the open crystal structure of apo *Tt* IPMDH.

[c] The fits for open/closed mixture were obtained by OLIGOMER, V_{open} and V_{closed} correspond to the volume fractions of each state found by OLIGOMER.

The minimum values of discrepancy (in bold) indicate the best correlation between SAXS data and crystallographic model.

The small variations in the calculated molecular mass are due to different numbers of residues resolved in different crystal structures.